



Calhoun: The NPS Institutional Archive

Faculty and Researcher Publications

Faculty and Researcher Publications

2004

LWIR spectral measurements of volcanic sulfur dioxide plumes

Mares, A.G.

Mares, A.G., Olsen, R.C., Lucey, P.G., LWIR spectral measurements of volcanic sulfur dioxide plumes, Algorithms and Technologies for Multispectral, Hyperspectral, and Ultraspectral



Calhoun is a project of the Dudley Knox Library at NPS, furthering the precepts and goals of open government and government transparency. All information contained herein has been approved for release by the NPS Public Affairs Officer.

**Dudley Knox Library / Naval Postgraduate School
411 Dyer Road / 1 University Circle
Monterey, California USA 93943**

<http://www.nps.edu/library>

LWIR Spectral measurements of volcanic sulfur dioxide plumes

A.G. Mares^{1*}, R. C. Olsen¹, P. G. Lucey²

¹Physics Department, Naval Postgraduate School, Monterey, CA 93943

²IGPP, University of Hawai'i at Manoa, Honolulu, HI 96822

ABSTRACT

This work examines the process of detecting and quantifying volcanic SO₂ plumes using the Airborne Hyperspectral Infrared Imager (AHI) developed by the University of Hawaii. AHI was flown over Pu'u'O'o Vent of Kilauea Volcano in Hawaii to collect data on SO₂ plumes. AHI is a LWIR pushbroom imager sensitive to the 7.5 - 11.5 μ region. Spectral analysis and mapping tools were used to identify and classify the SO₂ plume in both radiance and emissive space. MODTRAN was used to model the radiance observed by the sensor as it looked to the ground through an SO₂ plume. A spectral library of radiance profiles with varying ground surface temperatures and SO₂ concentrations was developed, and the AHI data fitted to the varying model profiles. Reasonable values of SO₂ emission were obtained.

1. INTRODUCTION

There is an ongoing need to monitor volcanic activity, including a desire to monitor the output of sulfur dioxide (SO₂). During periods of sustained eruption, Kilauea emits about 2,000 tons of sulfur dioxide gas (SO₂) each day. There are many reasons for monitoring the amount of SO₂ emitted from Kilauea. SO₂ is a poisonous gas that can irritate human respiratory systems. It also reacts with oxygen and water in the atmosphere to produce volcanic smog (vog) and acid rain¹. In addition to better understanding the affects it may have on the health and welfare of the people of Hawaii, the SO₂ emission rate is also monitored with the belief that it can also aid in predicting periods of increasing or decreasing activity within the volcano². A wide range of airborne and spaceborne remote sensing instruments that have been applied to aid in the study of volcanoes, ranging from UV to LWIR.³ The work reported here is from LWIR spectral measurements taken with an imaging sensor at high spatial resolution. The work is most comparable to earlier work with the TIMS instrument, but with significantly higher spectral resolution.⁴ The focus of this paper is a set of observations collected by the AHI LWIR imaging spectrometer over Kilauea on April 18, 2002. These observations resulted in quantitative estimates of SO₂ production.

1.1 Instrumentation

The University of Hawaii's Hawaii Institute of Geophysics and Planetology (HIGP) designed and built AHI as part of the Defense Advanced Research Projects Agency's (DARPA) Hyperspectral Mine Detection (HMD) program. The main goal of the program was to develop and demonstrate a hyperspectral infrared capability for remote buried mine detection. The program outlined several high level system and sensor requirements based on an extensive phenomenology measurement program that guided the design and construction of AHI.⁵

The most pertinent characteristics are:

- Spectral Range: 8.3 – 11 microns
- Spectral Resolution: <32 wavenumbers
- Noise Equivalent Spectral Radiance (NESR): < 0.01 watt/m²-micron-sr at 300 K

The telescope is a two-element diffraction limited transmission lens with a 111-micron focal length and 35 mm aperture. The spectrograph is an uncooled commercial reflective f/4 imaging spectrograph with gold-coated optics. It is a grating spectrograph that has a linear dispersion at the output. An uncooled spectrograph is possible due to the sensor's background suppressor. The background suppressor cools the FPA, a three-element transmission reimaging system, and a linear variable filter that are all housed in a vacuum dewar. The FPA is a 256 by 256 Rockwell TCM2250 HgCdTe array sensitive to an LWIR band from 7.5 to 11.5 microns. It is cooled to 56 degrees Kelvin (K) by

* Aimee.Mares@osd.mil, olsen@nps.navy.mil

a 1.5 watt split Stirling mechanical cryocooler. At 56 K, the half power drop-off in sensitivity is at 11.5 microns. The array is operated at its maximum frame rate of 150 Hz with an integration time of 3 milliseconds in order to avoid saturation for scenes that may contain temperatures of 70 degrees Celsius. A separate 0.1 liter liquid nitrogen reservoir cools the sensor's optics. AHI operates as a pushbroom scanner.⁵

2. OBSERVATIONS

2.1 AHI Flight Lines

AHI collected data between the hours of 9:00 and 11:00 AM on April 18, 2002. A map of the flight lines is displayed in Figure 1. The aircraft flew at an altitude of 4000-4500 ft. Weather observations for these two hours were obtained from the weather station at the Hilo Airport, approximately 37.5 km north of Pu'u'O'o and at an elevation of 44 feet above mean sea level. Between these hours the station reported clear skies with a few scattered clouds, an average surface air temperature of 26.7 degrees Celsius, a relative humidity of 68 percent, and a barometric pressure of 1013.55 millibars. The winds were very light and variable out of the east-southeast.

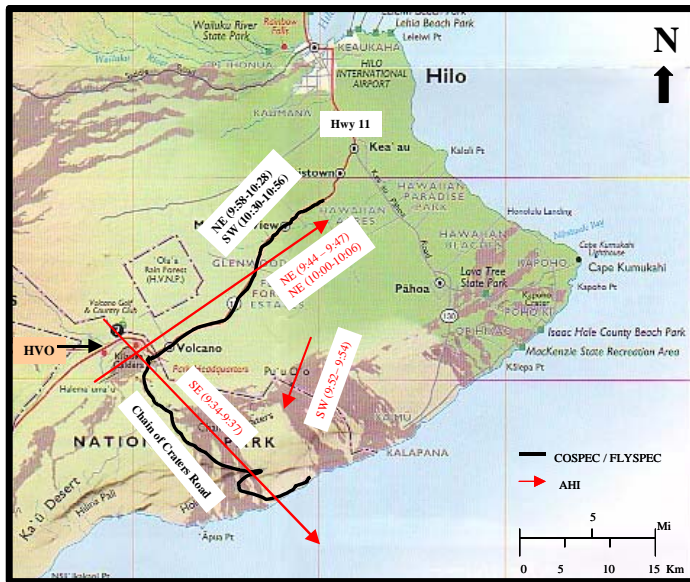


Figure 1. Flight path's for AHI, location of Chain of Craters Road, Pu'u'O'o vent, Hawaiian volcano observatory (HVO). The flight line of interest is the one on the lower right, up the hill from Kalapana, at 0953 local time.

Most of these conditions were ideal with the exception of the winds. Ideal wind speeds and directions for data collection on the Pu'u'O'o plume are northeasterly trade winds with a consistent speed of 5 m/s. These ideal wind conditions normally carry the plume from Pu'u'O'o down over the Chain of Craters Road. The east-southeast winds of April 18 carried the winds over Highway 11. This was unfortunate, because it made coincident UV measurements made from the road useless for calibration and comparison purposes. The SO₂ plume basically rose vertically, presenting a very dense plume in very localized region. The nature of the UV data are discussed elsewhere.⁶ The light and variable speeds also caused some problems for the analysis of an emission rate for the data collected, as a steady and consistent wind speed is one of the main variables in this calculation.

2.2 AHI Observations

Figure 2 displays two pictures of the Pu'u'O'o Vent of Kilauea Volcano in Hawaii. The picture on the left is a visible image of the vent taken from an aerial view looking west-southwest. The picture on the right is an LWIR image of the vent taken by AHI mounted on a twin-otter airplane traveling west-southwest. Note that this image is a fairly narrow strip, passing over the vent. The LWIR image is bright over the higher temperature regions.



Figure 2. Visible and Infrared Image of Pu'u'Ō'o Vent of Kilauea Volcano, Hawaii, Collected on April 18, 2002. Flight line image has been compressed in the flight line direction for presentation purposes.

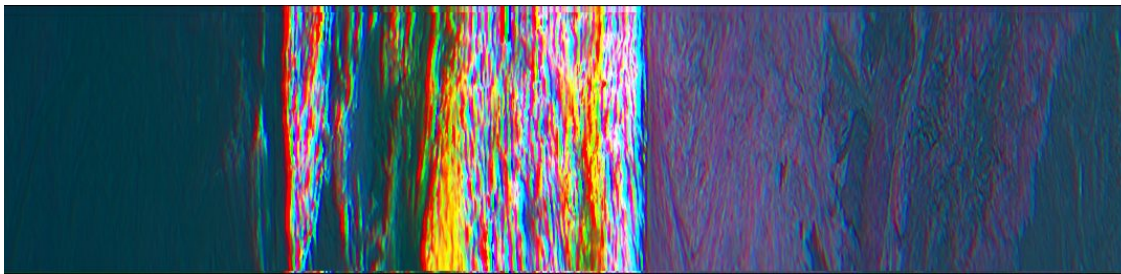


Figure 3. Decorrelation stretch presentation of AHI image taken on flight line starting at 095349. Data set is 256 samples x 1436 lines; the image is truncated on the right for lack of interesting data. The yellow regions in this presentation are the regions with SO₂. This figure is rotated 90° CCW with respect to the radiance image on the right of figure 2.

Analysis began by casting the data into a TIMS format, in order to reproduce the approach previously used by Realmuto et al.^{4,7}. The 205 spectral bands were resampled down to the 6 TIMS bands, and then presented as an RGB triple for TIMS bands 5, 3, and 2, respectively (wavelengths of 10.7, 9.2, and 8.8 μ). The 8.6-8.8 micron band is sensitive to a significant SO₂ absorption feature, and hence regions with significant SO₂ concentration appear yellow. The technique is a powerful method for quickly reviewing the data. Figure 3 shows the pass over the Pu'u'Ō'o vent which was analyzed in depth. The bright yellow stripes (vertical in Figure 3) show the regions of high SO₂ concentration. All the scenes taken were reviewed in this way, with the illustrated data set presenting the one successful observation on this data.

Several approaches to analysis were then followed. Traditional spectral techniques such as principal component transforms were applied. Various visualization techniques were then applied to the transformed data, in order to determine what sorts of unique spectra were contained in the data set. This allowed the data set to be decomposed into a modest number of spectrally distinct regions. Characteristic spectra from several regions are illustrated in Figure 4. Three spectra are shown from regions believed to have very little SO₂, taken over ground regions at significantly different temperatures. The remaining spectra exhibit the rather dramatic SO₂ absorption feature.

3. ANALYSIS

The first approach to analysis followed previous patterns evolved for surface studies⁸. Given the relatively modest character of atmospheric absorption features in the data set (aside from the volcanic plumes), it seemed reasonable to look at the spectra by assuming that plume effects were not great above 10 μ , and fit blackbody curves to the higher wavelength data. The normalized emissivity can then be obtained by dividing out the blackbody spectra. This requires an assumption about the emissivity of the soil – we took $\epsilon = 0.96$ for these calculations.

Figure 5 displays both the radiance comparison and corresponding emissivity profiles generated for a 3 x 3 pixel average around several characteristic pixels. Note the unusually high temperatures for the background. The modeled ‘soil’ temperature ranged up to 425K. The emissivity plots show that the absorption feature is rather dramatic – much larger than the 90-95% fluctuations more routinely found in soil studies. The temperature analysis approach was validated to some extent by application to ocean water data taken at the end of one of the flight lines. The next step is to model the plume.

Unfortunately, the spectral imagery problem here differs from work previously done with terrestrial observations⁸. We are normally allowed to know something about the ground – that is the temperature and emissivity. In previous work, we have been able to depend on the presence of ground vegetation, which provides a calibration standard that can be used to extract atmospheric effects. You can generally assume fairly benign environmental features – slowly varying atmosphere, slowly varying temperatures, etc. None of these features define our current data set.

The ground below the plume varies significantly in radiance, while the plume itself is characterized by significant variations in composition within the scene.

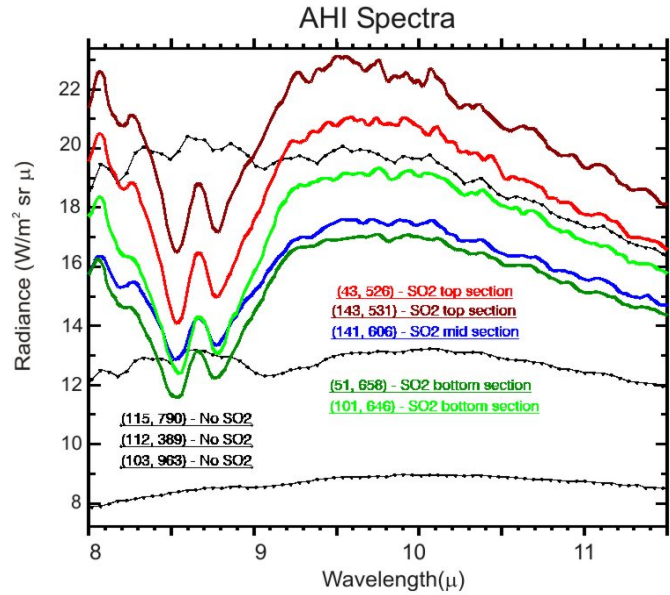


Figure 4. Characteristic radiance spectra taken from the flight line illustrated in Figure 3. Note the strong absorption feature from 8-9 μ .

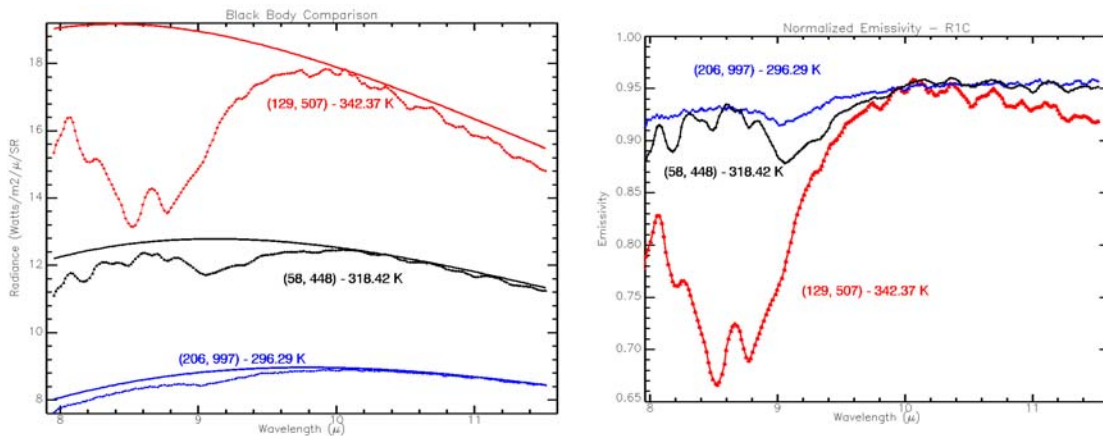


Figure 5. Radiance data overlapped with blackbody curves matched to the long-wavelength portion of the observed data. The emissivity of the background is assumed to be 0.96.

3.1 MODTRAN model

The modeling approach developed for this work was to use MODTRAN, the standard atmospheric modeling code⁹. We used MODTRAN 4.0, release 2, running under Windows 2000. Quoting from Realmuto et al, 1997, “MODTRAN calculates atmospheric transmission and radiance using models of the absorption bands of 12 gas molecules (H₂O, CO₂, O₃, N₂O, CO, CH₄, O₂, NO, SO₂, NO₂, NH₃ and HNO₃), utilizing three-parameter band models with spectral resolutions of 1 cm⁻¹.”⁴

The model was applied using the US Standard atmosphere model (1976), modified for the SO₂ layer. We ran the model with 4 layers between the surface and the sensor. The initial layer is developed from the ground to the altitude of the top of the plume. The temperature, pressure, and relative humidity of this layer are taken from the weather reports from the Hilo weather station during the hours of collection. This is also the layer where the SO₂ concentration of the plume is defined. Two important assumptions relating to the SO₂ plume are made in the development of this layer. First, an assumption is made regarding the altitude and the thickness of the plume. As R1_C_095349 is an image collected directly over the vent, it is assumed that the altitude of the plume is at the surface of the vent or the very bottom layer in the atmospheric profile. As no direct measurements on the thickness of the plume were collected, an estimate of 150 m is used. Second, it is assumed that the temperature of the plume is in thermal equilibrium with the particular layer of the atmosphere in which it is described. The remaining three layers of the model are divided between the top of the plume and the altitude of the sensor. The standard atmospheric model is used to define the temperature, pressure, relative humidity, and atmospheric constituents of these layers. In retrospect, the assumption on the temperature of the plume was probably a poor one.

A series of MODTRAN model radiance files was created for varying ground temperatures and SO₂ concentrations. These were then fitted to the observations manually (by inspection). This was done for a variety of pixels in regions that were determined via spectral analysis. The spectral analysis process followed the standard principal components, interactive analysis approach normally used for ground studies^{6, 8, 10}. The process allowed us to identify spectrally significant areas. Figure 6 shows the different regions, and indicates the wide variety of pixel locations selected for analysis.

The profiles were initially examined for fit in the longer wavelength region (9.5 – 11.5 μm). This region is unaffected by SO₂ and can be used to examine the profile in terms of temperature. Adjustments to the ground surface temperature input were made if an ideal fit was not observed. After a proper fit was established in the longer wavelengths, the SO₂ concentration was adjusted to develop the best fit to the SO₂ signature seen in the AHI data. Figure 7 illustrates one such fit for a spot in the red band in the lower region of the figure to the right. For each such point, an average over a 5x5 pixel group was used.

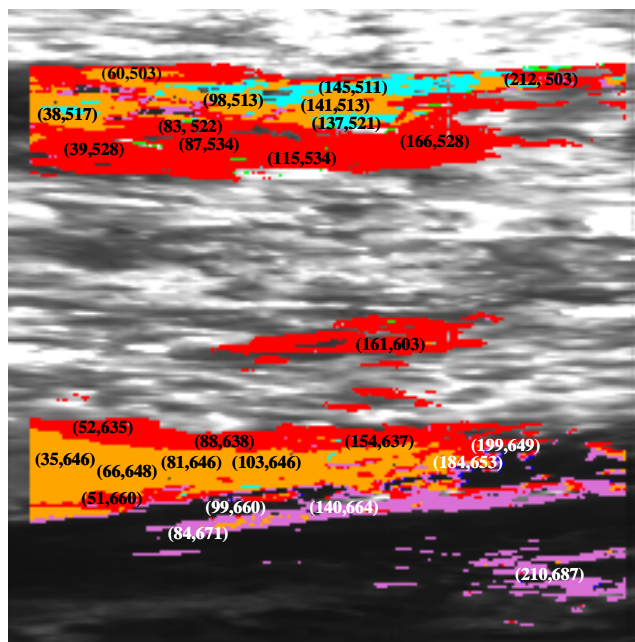


Figure 6. Radiance Image With Final SO₂ Classes Annotated

Note that there is a small offset in the absorption feature wavelength. This was a persistent characteristic of our analysis. This analysis was conducted for each pixel class, and for a range of pixels within each class which had been separated in our spectral analysis. As an illustration of the range of parameters produced by this analysis, Table 1 gives the range of parameters. The terms upper plume and lower plume refer to the y values indicated in Figure 6, and the relative position within that figure. The other main class that is represented here is the “orange” class, as indicated in Figure 6. The range of values found for those pixel groups are given in Table 2. Temperatures are similar for the two

regions; the main difference is a higher SO₂ concentration in the second spectral class. Somewhat similar values were found for the “orchid” class which lies along the bottom portion of Figure 6.

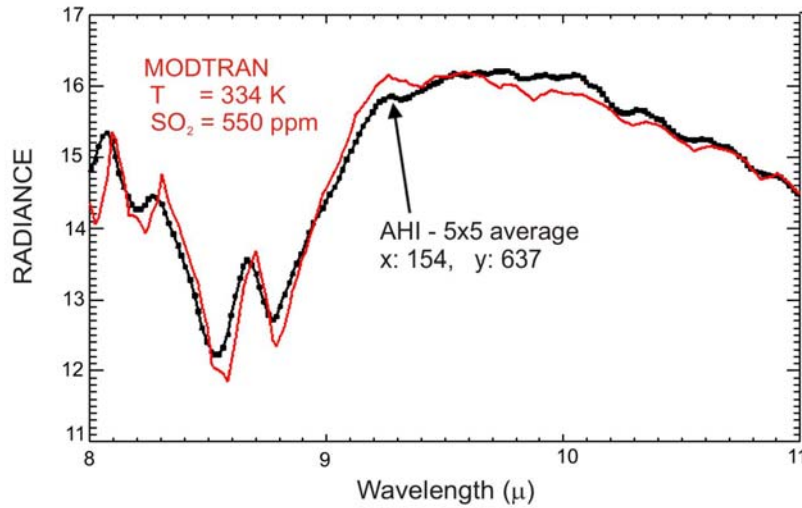


Figure 7. MODTRAN analysis for AHI data.

Table 1

Red Class SO2	deg K or ppm	Plume Section
Max Temp	363 K	Upper
Min Temp	335 K	Lower
Max SO2	725 ppm	Lower
Min SO2	325 ppm	Lower

Table 2

Orange Class SO2	deg K or ppm	Plume Section
Max Temp	350 K	Lower
Min Temp	343 K	Upper
Max SO2	1400 ppm	Upper
Min SO2	850 ppm	Lower

4. CONCLUSIONS

The imaging spectrometer data provided a significant new ability in mapping the volcanic plumes coming from Kilauea. The analysis process applied to the AHI data produced SO₂ concentrations ranging from 300-1500 ppm. The analysis seems fairly clear, but there is no way to test these values against ground truth for this collection, due to the unfortunate wind conditions. The offset in MODTRAN spectra for the SO₂ absorption feature is probably due to our temperature assumption for the volcanic plume. A warmer plume would explain the offset.

Future work involving a reflight of AHI is hoped for. We will again attempt to obtain cooperative measurements using the conventional UV measurement standards, and should be able to obtain these with more favorable winds. It appears that some attempt to estimate the plume temperature is in order.

REFERENCES

1. Sutton, J., Elias, T., Hendley, J., and Stauffer, P., "Volcanic Air Pollution—A Hazard in Hawaii", U.S. Geological Survey Fact Sheet 169-97, June 2000. <http://wrgis.wr.usgs.gov/fact-sheet/fs169-97>
2. Sutton, A., Elias, T., Gerlach, T., and Stokes, J., "Implications for eruptive processes as indicated by sulfur dioxide emissions from Kilauea Volcano, Hawaii, 1979 – 1997," *Journal of Volcanology and Geothermal Research*, no. 108, pp. 283-302, 2001.
3. Mouginis-Mark, P., Crisp, J., and Fink, J., *Geophysical Monograph 116, Remote Sensing of Active Volcanism*, American Geophysical Union, 2000.
4. Realmuto, V., Sutton, A., Elias, T., "Multispectral thermal infrared mapping of sulfur dioxide plumes: A case study from the East Rift Zone of Kilauea Volcano, Hawaii," *Journal of Geophysical Research*, vol. 102, no. B7, pp. 15057-15072, 1997
5. Lucey, P., Williams, T., Mignard, M., Julian, J., Kobubun, D., Allen, G., Hampton, D., Schaff, William, Schlangen, M., Winter, E., Kendall, W., Stocker, A., Horton, K., and Bowman, A., "AHI: an airborne long-wave infrared hyperspectral imager," *SPIE Proceedings*, vol. 3431, pp. 36-43, November, 1998.
6. Mares, A. G., *Remotely Sensed Density Measurements Of Volcanic Sulfur Dioxide Plumes Using A Spectral Long Wave Infrared Imager*, Master's Thesis, Naval Postgraduate School, September 2002.
7. Realmuto, V., Abrams, M., Fabrizia, V., and Pieri, D., "The use of multispectral thermal infrared image data to estimate the sulfur dioxide flux from volcanoes: A case study from Mount Etna, Sicily, July 29, 1986," *Journal of Geophysical Research*, vol. 99, no. B1, pp. 481-488, 1994.
8. Collins, B. H., R. C. Olsen, J. Hackwell, *Thermal Imagery Spectral Analysis, Imaging Spectrometry III, SPIE Proceedings Volume 3118*, pp-94-105, 1997.
9. Berk, A., Anderson, G., Acharya, P., Chetwynd, J., Bernstein, L., Shettle, E., Matthew, M., and Adler-Golden, S., *MODTRAN4 User's Manual*, Air Force Research Laboratory, Space Vehicles Directorate, Hanscom AFB, MA, June, 1999.
10. Stefanou, M. S., Olsen, R. C., and Cristi, R., *A Signal Processing Perspective of Hyperspectral Imagery Analysis Techniques*, Master's Thesis, Naval Postgraduate School, Monterey, California, June 1997.